Acta Oceanol. Sin., 2022, Vol. 41, No. 6, P. 12–21
https://doi.org/10.1007/s13131-021-1930-z
http://www.aosocean.com
E-mail: ocean2@hyxb.org.cn

Radium-traced nutrient outwelling from the Subei Shoal to the Yellow Sea: Fluxes and environmental implication

Jian'an Liu[1], Dongyan Liu[1], Jinzhou Du[1]*

[1] State Key Laboratory of Estuarine and Coastal Research, East China Normal University, Shanghai 200241, China

Received 26 January 2021; accepted 19 April 2021

Abstract

The Subei Shoal is the largest sandy ridge in the southern Yellow Sea and is important source for nutrient loading to the sea. Here, the nutrient fluxes in the Subei Shoal associated with eddy diffusion and submarine groundwater discharge (SGD) were assessed to understand their impacts on the nutrient budget in the Yellow Sea. Based on the analysis of ^{223}Ra and ^{224}Ra in the field observation, the offshore eddy diffusivity mixing coefficient and SGD were estimated to be 2.3×10^8 cm^2/s and 2.6×10^9 m^3/d (16 cm/d), respectively, in the Subei Shoal. Combined the significant offshore decreasing gradients of nutrient in seawater of the Subei Shoal, the spatially integrated nutrient outwelling fluxes to the Yellow Sea were 262–1 465 μmol/(m^2·d) for DIN, 5.2–21 μmol/(m^2·d) for DIP and 711–913 μmol/(m^2·d) for DSi. Compared to the riverine input, atmospheric deposition and mariculture, nutrient outwelling from the Subei Shoal might play an important role in nutrient budget of the Yellow Sea. These nutrient fluxes could provide 4.1%–23% N and 1.3%–5.3% P requirements for the primary productivity, and the deviated DIN/DIP ratios have the potential to affect the growth of phytoplankton in the marine ecosystem of the Yellow Sea.

Key words: nutrient outwelling, eddy diffusion, submarine groundwater discharge, radium isotopes, Subei Shoal, Yellow Sea

Citation: Liu Jian'an, Liu Dongyan, Du Jinzhou. 2022. Radium-traced nutrient outwelling from the Subei Shoal to the Yellow Sea: Fluxes and environmental implication. Acta Oceanologica Sinica, 41(6): 12–21, doi: 10.1007/s13131-021-1930-z

1 Introduction

Nutrient concentrations and their ratios have been proved as one of the crucial indicators for health assessment of the ecological environment, especially in the coastal marine ecosystem. Coastal zone receives a large amount of nutrient from multiple sources, such as atmospheric deposition, riverine input and submarine groundwater discharge (SGD) (Anderson et al., 2002; Moore, 2010). Therefore, the coastal ecosystems are hotspots for nutrient accumulation, biological growth, and laterally outwelling nutrient to the open ocean (Andersen and Conley, 2009; Charette et al., 2007; Su et al., 2013b). This nutrient outwelling from coastal zone significantly elevates the oceanic nutrient level and changes the nutrient structure of the water ecosystems, which probably contribute to the occurrence of eutrophication, harmful algal blooms and hypoxia (Le Moal et al., 2019; Tang et al., 2004; Zhang et al., 2007a). For example, Kwon et al. (2019) suggested that nutrients transported horizontally from inner-shore waters were fueling the spread of dinoflagellate red tides along the coast of Korea.

In the coastal waters, nutrient cycles are mainly controlled by external supplements and internal biogeochemical cycles, in which external sources transport significant nutrient into the coastal zones and then involve in ecological and biogeochemical functions with the loss of nutrient (Falkowski et al. 1998; Walsh, 1991). Besides, the coastal waters also exchange numerous nutrients with the open ocean due to the water mixing, but attention cannot be paid to the processes. The primary mechanism behind nutrient is advection and diffusion movement from the coastal region to the open ocean, in which eddy diffusion as the main water mixing process could significantly contribute to the fate of nutrient (Pasquero, 2005; Su et al., 2013b). Previous studies revealed the importance of SGD for delivering nutrient into the coastal regions (Liu et al., 2018; Zhang et al., 2020a), whereas the contributes of nutrient outwelling through eddy diffusion processes from the coastal zone are still poorly understood (Su et al., 2013a; Su et al., 2013b). Especially in the river poorly-influenced coastal zone, eddy diffusion could act as the essential driver for nutrient moving from coastal waters to open ocean, however, very limited studies have demonstrated the significance of this process.

Due to the complex processes of water mixing, quantification of the eddy diffusion associated nutrient outwelling to the coastal ocean is challenging. In early stage, eddy diffusivity was determined by satellite remote sensing (Fischer, 1980) and numerical simulation (Werner et al., 1993), but it is difficult for wide calculation under the characteristic of small-scale temporal and spatial variability. Fortunately, radium isotopes have been shown to be useful tracers to access water movements, such as eddy diffusion and SGD, and fluxes of dissolved nutrient from the coastal zone to the ocean (Moore, 1996, 2000; Su et al., 2013a; Wang et al., 2018). Radium isotopes are produced by the decay of their parent U-Th series nuclides from sediment and/or soil in the rivers

Foundation item: The National Science and Technology Major Project of the Ministry of Science and Technology of China under contract No. 2016YFC1402106; the National Natural Science Foundation of China under contract Nos 41376089, 41576083, 41976040, 41876127 and 42030402; the China Postdoctoral Science Foundation under contract No. 2020M671048.
*Corresponding author, E-mail: jzdu@sklec.ecnu.edu.cn

or the continental shelf and then transport to offshore seawater (Li et al., 1977; Swarzenski, 2007). There are four naturally occurring radium (Ra) isotopes, that is, ^{224}Ra, ^{223}Ra, ^{228}Ra and ^{226}Ra, are radiogenic with half-lives of 3.66 d, 11.6 d, 5.75 a and 1 600 a, respectively, which provide the information of water mixing processes on scales from days to years (Moore, 2000). Radium isotopes could be used to not only calculate advection and eddy diffusivity (Ku and Luo, 1994; Li and Cai, 2011), but also obtain SGD flux (Moore, 2010), and could also effectively avoid the influence of biological process (Sarmiento et al., 1990). Therefore, radium isotopes can give insights into the nutrient outwelling through eddy diffusion processes to the ocean.

Since 2007, the world's largest green tides bloom occurred annually in the Yellow Sea (Liu et al., 2009a; Liu et al. 2016), and were recognized to be originated from the southwestern Yellow Sea near the coast of Jiangsu Province, which is called the Subei Shoal (Liu et al., 2013). As the essential biogenic element for phytoplankton growth in seawater, high nutrient, especially nitrogen levels, were considered as one of the most significant contributors to the development of green tides in the Subei Shoal (Li et al., 2015; Zhang et al., 2020b). Due to the unique features, which are broad tidal flats, elongated sand ridges and grooves and strong tidal forces, the Subei Shoal is a traditional aquaculture base for the *Porphyra* crops (Bao et al., 2015; Xiao et al., 2020). Meanwhile, the Subei Shoal is receiving a large amount of nutrient-rich SGD and it elevates the nutrient level in the seawater that may fuel green tides (Liu et al., 2017; Zhao et al., 2018). Therefore, the geochemical and ecological environment of the Subei Shoal is expected to influence or even regulate the ecosystem of the Yellow Sea (Xiao et al., 2020).

Previously, Men et al. (2006) used ^{228}Ra to calculate horizontal eddy diffusion coefficient within 200 km offshore in the western Yellow Sea, and then Su et al. (2013b) in our laboratory estimated the horizontal transport of nutrient within 500 km offshore of the Yellow Sea combined ^{223}Ra and ^{226}Ra. However, later Moore (2015) indicated that it was inappropriate to model water mixing rates utilizing ^{226}Ra and ^{228}Ra in the coastal zone within 500 km offshore. Moreover, the previous study cannot evaluate the contribution of the Subei Shoal region. Therefore, this study, examined radium isotopes and nutrient in the Subei Shoal, aiming to quantify SGD-derived nutrient fluxes into the Subei Shoal, and the nutrient outwelling through eddy diffusion to the Yellow Sea, and evaluate the potential influence on harmful algal blooms in the Yellow Sea. Based on these results, this study would provide insights into nutrient transporting processes in the Subei Shoal and improve the knowledge of the biogeochemical process of water movement.

2 Materials and methods

2.1 *Study area and sampling procedures*

A field observation was carried out in the Subei Shoal in the southern Yellow Sea during March 23–31, 2017. The Subei Shoal is located off the coast of southeastern Jiangsu Province and is highly sensitive to a temperate monsoon climate. As the largest sandy ridge in the southern Yellow Sea, the water depth of the Subei Shoal is relatively shallow at approximately 12 m. Due to the strong tidal force, the Subei Shoal is well mixed and high turbid (Miao et al., 2020).

During this observation, radium isotopes and nutrient samples in seawater and coastal groundwater were collected, sampling stations were shown in Fig. 1. For radium isotopes, approximately 25 L seawater were collected using a submersible pump at 0.5–1 m depth, while coastal groundwater (~10 L) was obtained from a push-point piezometer using a peristaltic pump. The salinity was measured directly *in situ* using a pre-calibrated portable salinometer with multiple parameters (Germany, multi 350i). After collection, radium samples were filtrated to remove suspended particles and then allowed to pass through a cartridge that was filled with 20 g of MnO_2-impregnated acrylic fiber to enrich radium isotopes (Moore, 1976).

Corresponding to each radium sample, ~60 mL water for nutrient were filtered with acid pre-cleaned 0.45 μm pore-size acetate cellulose filters into polyethylene bottles, and then the water samples were poisoned with saturated $HgCl_2$ and stored in the dark.

2.2 *Radium isotopes and nutrient analysis*

After preparation, the cartridge with Mn-fiber was immediately placed in the shipboard radium delayed coincidence counter (RaDeCC) to measure ^{224}Ra (Moore and Arnold, 1996). Each sample was again measured a week after collection to determine ^{223}Ra, and 5 weeks after collection all the samples were analyzed for ^{228}Th on the same instrument to correct for suppor-

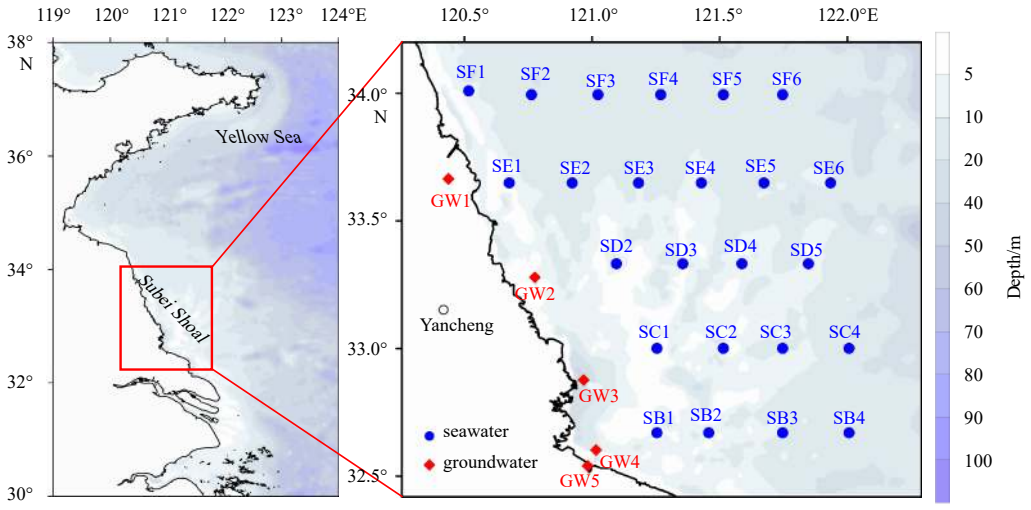

Fig. 1. Study area and sampling stations in the Subei Shoal during March 2017.

ted ^{224}Ra (Moore, 2008). The uncertainties of ^{223}Ra and ^{224}Ra were estimated to be approximately 20% and 8%, respectively, using the equations reported in Garcia-Solsona et al. (2008).

Nutrient concentrations were quantified with an auto-analyzer (Model: Skalar SANplus). The concentration of dissolved inorganic nitrogen (DIN) is the sum of NO_3^-, $NO_2^-$and NH_4^+. dissolved inorganic phosphorus (DIP) and dissolved inorganic silicon (DSi) represent the concentrations of PO_4^{3-} and SiO_3^{2-}, respectively. The analytical precisions of NO_2^-, NO_3^-, NH_4^+, PO_4^{3-} and $Si(OH)_4$ were all better than 5% and the detection limits were 0.01 μmol/L, 0.05 μmol/L, 0.05 μmol/L, 0.01 μmol/L and 0.1 μmol/L, respectively.

2.3 *SGD flux*

This study would quantify the SGD flux based on ^{224}Ra mass balance model that has been widely applied (Garcia-Orellana et al., 2014; Liu et al., 2018). Under steady state system, the input of ^{224}Ra fluxes into the system equal to losses from the system (Moore, 1996). Therefore, by estimating all the sources and sinks of ^{224}Ra except for SGD, ^{224}Ra flux derived from SGD could be obtained. Subsequently, combined with ^{224}Ra activity in coastal groundwater, this study could access the SGD flux. For these, the equation used for calculating SGD flux is expressed as

$$F_{\mathrm{SGD}} = \frac{C_{\mathrm{SW}}\cdot V\cdot\lambda+\frac{(C_{\mathrm{SW}}-C_{\mathrm{ocean}})\cdot V}{\tau}-F_{\mathrm{riv}}\cdot C_{\mathrm{riv}}-F_{\mathrm{sed}}\cdot A-\frac{C_{\mathrm{des}}\cdot C_{\mathrm{SPM}}\cdot V}{\tau}}{C_{\mathrm{GW}}}, \quad (1)$$

where F_{SGD} refers to the flux of SGD; C_{SW} is ^{224}Ra activity in seawater of the study area; C_{ocean} is ^{224}Ra activity in seawater of ocean in the Yellow Sea; C_{riv} is ^{224}Ra activity in surrounding rivers; C_{des} is ^{224}Ra activity desorbed from suspended particulate matter (SPM); C_{GW} is ^{224}Ra activity in coastal groundwater; τ refers to water residence time in the study region; F_{riv} refers to the freshwater discharge of rivers; F_{sed} refers to ^{224}Ra diffusion rate from sediment; C_{SPM} refers to the concentration of SPM in seawater; V refers to the water volume of the study area; and A refers to the area of the study region.

2.4 *Offshore mixing*

Considering the water residence time in the study area is on the scale of the week, this study would apply the short half-lives isotopes of ^{223}Ra and ^{224}Ra to estimate eddy diffusivity and advection rates (Moore, 2015; Zhao et al., 2018). Assuming the study area is in a steady state and there is no additional input of radium isotopes beyond the nearshore other than those constrained by benthic diffusion, and the water body in the study region is situated over the mean lifetimes of ^{223}Ra and ^{224}Ra, a fully-resolved 1 D advection–diffusion equation is built by combining ^{223}Ra and ^{224}Ra (Moore, 2000; Sippo et al., 2019; Su et al., 2013a), in which is shown as

$$\left.\begin{aligned} K_{\mathrm{h}}A_{223}^2+w_xA_{223}=\lambda_{223}\\ K_{\mathrm{h}}A_{224}^2+w_xA_{224}=\lambda_{224}\end{aligned}\right\}, \quad (2)$$

where x refers to the distance to the coastline; K_{h} and w_x are offshore eddy diffusivity mixing coefficient and offshore advection rate; λ_{223} and λ_{224} are the decay constants of ^{223}Ra and ^{224}Ra, respectively; A_{223} and A_{224} are the index coefficients obtained by fitting the measured radium activities to a function with a form by

$$C_x = C_0\exp(-A\cdot x), \quad (3)$$

where C_x is radium activity at distance x; C_0 is initial radium activity along the coastline in coastal groundwater.

3 Results

3.1 *Radium*

During the observation, salinity in surface seawater ranged from 27.4 to 32.1 in the Subei Shoal, in which the lowest salinity occurred near to shore and decreased moving offshore (Fig. 2a). In surface seawater, ^{224}Ra and ^{223}Ra activities ranged from 1.5 Bq/m^3 to 32.0 Bq/m^3 and 0.13 Bq/m^3 to 1.40 Bq/m^3, with the average activities of (11.0±7.5) Bq/m^3 (n=24) and (0.50±0.31) Bq/m^3

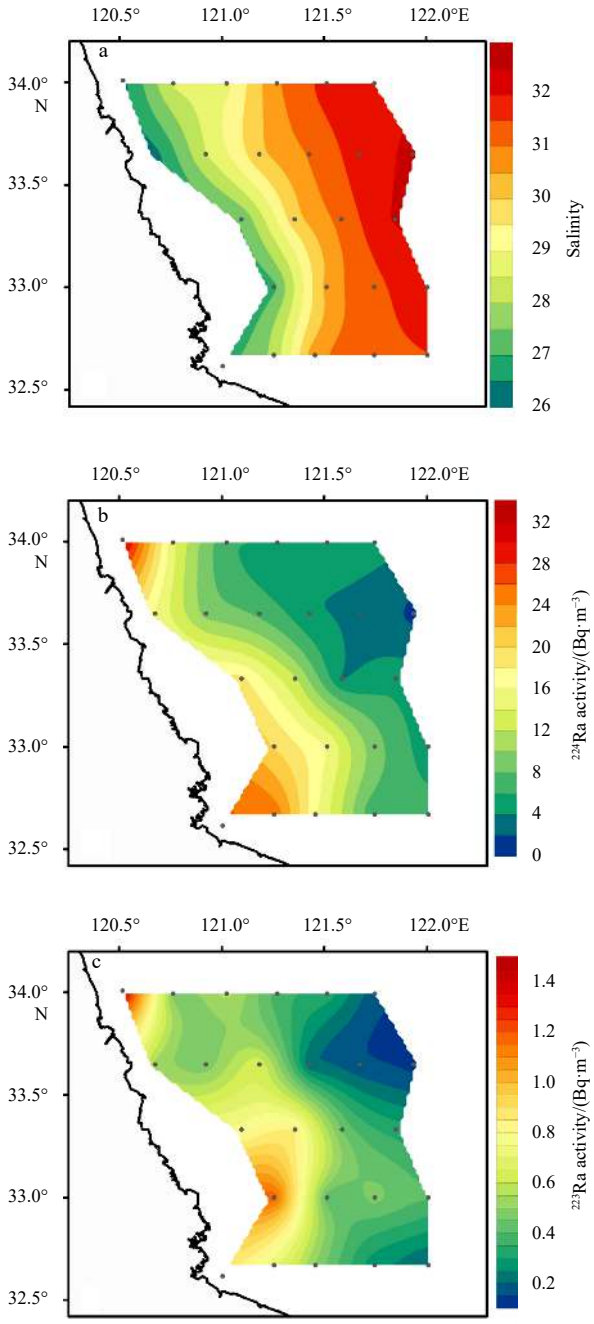

Fig. 2. Distributions of salinity (a), ^{224}Ra activity (b) and ^{223}Ra activity (c) in surface seawater of the Subei Shoal during the cruise of March 2017.

(n=24) , respectively. Similar to salinity, activities of ^{224}Ra and ^{223}Ra both showed significant decreasing trends from nearshore to offshore (Figs 2a–c). In nearshore within 60 km from the coastline, the mean ^{224}Ra and ^{223}Ra activities were (16.0±7.0) Bq/m^3 (n=12) and (0.71±0.30) Bq/m^3 (n=12), which were 3.1- and 2.4-fold higher than those in offshore (60 km) water (^{224}Ra: (5.2±1.8) Bq/m^3, n=12; ^{223}Ra: (0.29±0.11) Bq/m^3, n=12), respectively. Combining all the radium data in the Subei Shoal, the log-linear gradients of ^{224}Ra (n=24, R^2=0.80, $p<0.001$) and ^{223}Ra (n=24, R^2=0.76, $p<0.001$) were observed with the decreasing distance from the shoreline (Fig. 3). All these suggested that the primary radium source came from the shoreline that would be SGD (Moore, 2010), and after leaving near shore, the decreasing trend of ^{224}Ra and ^{223}Ra indicated the influence of radioactive decay and water mixing of the Yellow Sea.

In the coastal groundwater, the mean activities of ^{224}Ra and ^{223}Ra were (34±15) Bq/m^3 (n=5) and (1.40±0.42) (n=5) Bq/m^3, which were 3.2- and 2.7-fold of the activities in surface seawater of the Subei Shoal, indicating that coastal groundwater could be a dominated source of radium isotopes in surface seawater.

3.2 *Nutrients*

The nutrient analysis of the surface seawater revealed that DIN concentration ranged from 17 μmol/L to 59 μmol/L with an average of (30±10) μmol/L (n=24), DIP concentration ranged from 0.42 μmol/L to 1.2 μmol/L with an average of (0.70±0.20) μmol/L (n=24), and DSi concentration ranged from 6.5 μmol/L to 30 μmol/L with an average of (16±6.3) μmol/L (n=24). Nutrient concentrations in surface seawater both showed clear decreasing trends from nearshore water to offshore oceanic water (Fig. 4), suggesting that nutrients have similar sources with radium isotopes in the Subei Shoal. Within 60 km from the shoreline, the mean concentrations of DIN, DIP and DSi were (37±9.4) μmol/L, (0.81±0.18) μmol/L and (20±5.3) μmol/L, while concentrations in offshore (>60 km) water were (23±3.9) μmol/L, (0.59±0.14) μmol/L and (12±3.4) μmol/L, respectively. When plotting the nutrient concentrations in all samples versus distance from the shoreline, distinct linear relationships were observed for DIN (n=24, R^2=0.67, $p<0.001$), DIP (n=24, R^2=0.38, p=0.001 3) and DSi (n=24, R^2=0.69, $p<0.001$) (Fig. 5), also implied that coast would be the main source for nutrient in the Subei Shoal. Nutrient concentrations in coastal groundwater were 2.3, 2.0 and 9.0 times higher for DIN, DIP and DSi, respectively, which averaged of (68±50) μmol/L, (1.4±1.2) μmol/L and (142±102) μmol/L.

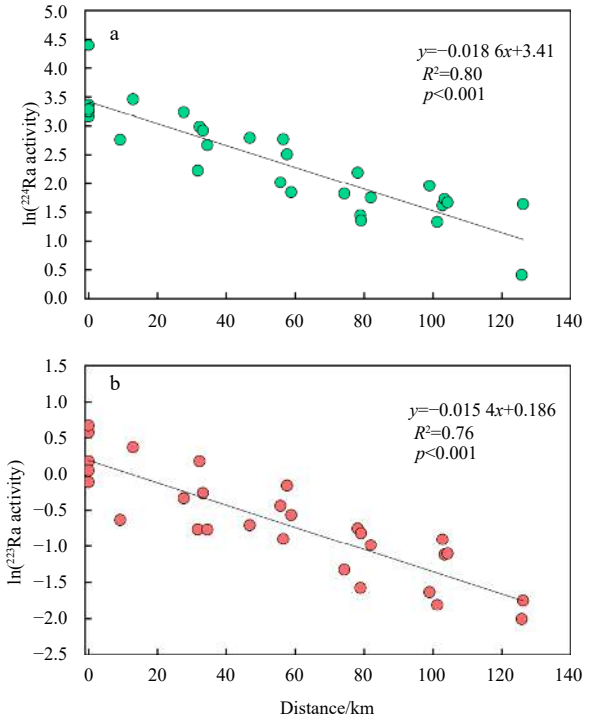

Fig. 3. Plots of ln of ^{224}Ra (a) and ^{223}Ra (b) activities in surface seawater vs. distance from the coastline in the Subei Shoal.

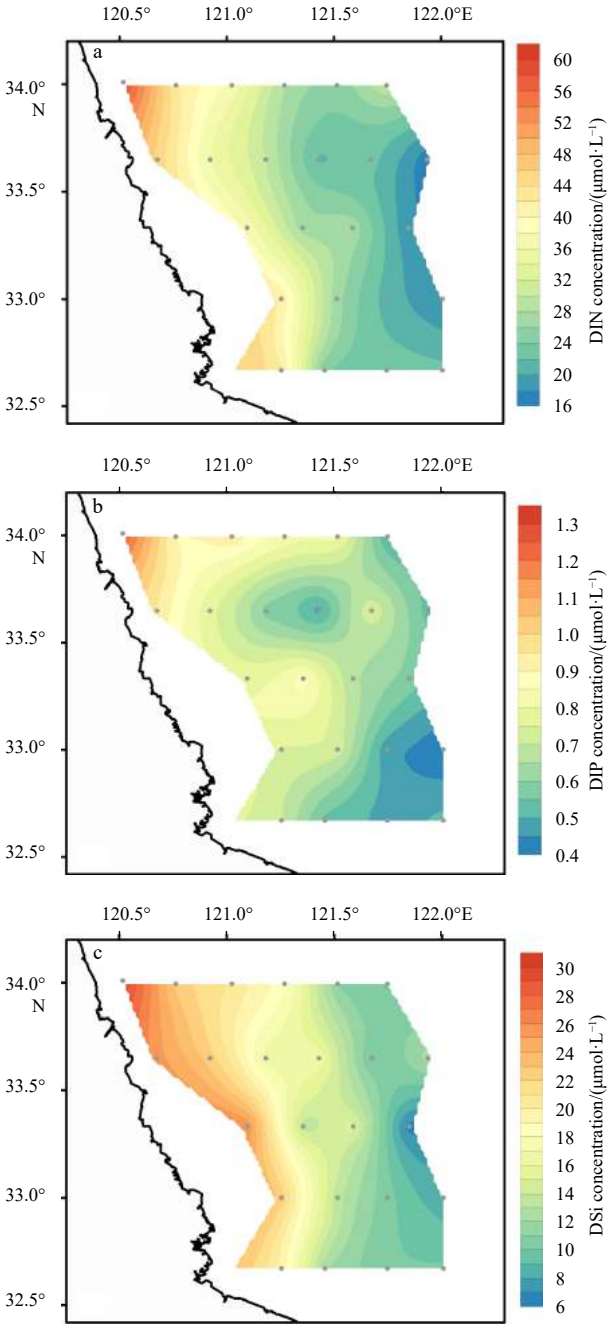

Fig. 4. Distributions of DIN (a), DIP (b) and DSi (c) concentrations in surface seawater of the Subei Shoal during March 2017.

3.3 *SGD flux*

Based on Eq. (1), a mass balance model based on ^{224}Ra was

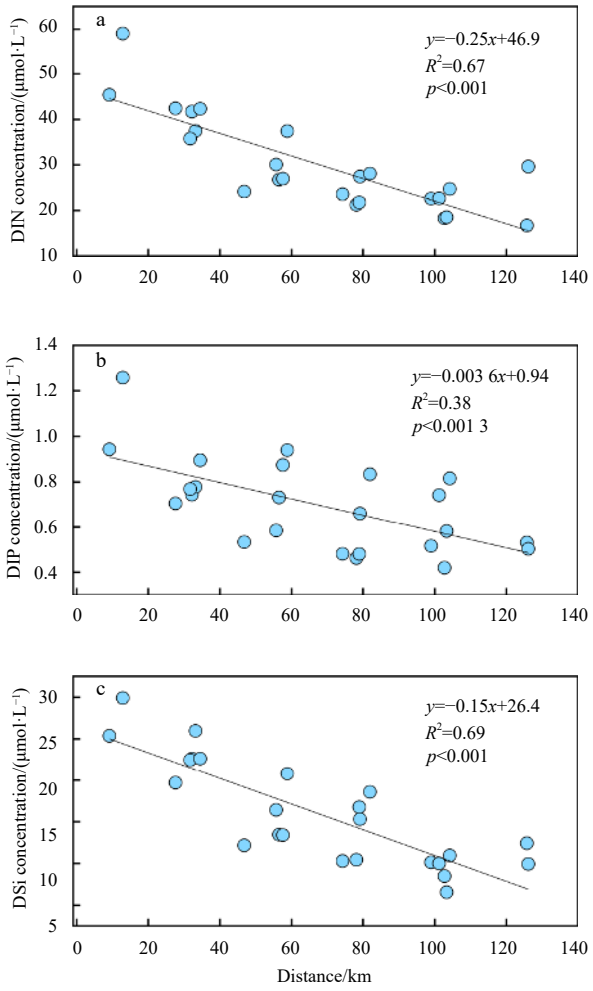

Fig. 5. Plots of DIN (a), DIP (b) and DSi (c) concentrations in surface seawater vs. distance from the coastline in the Subei Shoal.

established to calculate SGD flux in the Subei Shoal. As shown in Table 1, this study obtained each parameter, and the SGD flux was estimated to be 2.6×10^9 m^3/d. Normalized the SGD flux by area of the study region, the SGD rate could convert to be 16 cm/d.

3.4 *Eddy diffusion calculations*

Based on Eq. (2), this study used all the ^{224}Ra and ^{223}Ra data in the Subei Shoal to calculate offshore eddy diffusivity mixing coefficient and advection. With parameters shown in Table 2, this study estimated K_h and w_x in the study region to be 2.3×10^8 cm^2/s and −0.31 m/s. Additionally, this study divided all the radium stations into five transects, namely, transect SF to SB from north to south. Similar to all data, significant log-linear gradients of ^{224}Ra and ^{223}Ra activities were both observed from the five individual transects (Table 2). Therefore, using the same equation, this study obtained eddy diffusivity K_h ranged from 9.8×10^7 cm^2/s to 3.9×10^8 cm^2/s with an average value of 2.3×10^8 cm^2/s, advection w_x ranged from −0.048 m/s to −0.69 m/s with an average value of −0.33 m/s. The negative values of advection indicated onshore advection.

4 Discussion

4.1 *Eddy diffusivity*

As shown in Eq. (2), the 1 D advection–diffusion model was developed based on the assumptions of there is no additional radium input for the surface radium activity. Thus, the influence of benthic radium flux on eddy diffusivity should be negligible. In order to determine the potential impacts of benthic radium flux, this study used a simple method introduced in Su et al. (2013a), which deduced a parameter of β (d^{-1}), and obtained by

$$\beta = \frac{F_{sed}\cdot A}{V\cdot C_{SW}}. \tag{4}$$

In Eq. (4), the sediment diffusion fluxes of ^{223}Ra and ^{224}Ra were 0.24 Bq/(m^2·d) and 20 Bq/(m^2·d) (Gu, 2015; Liu et al., 2018). Therefore, this study calculated β_{223} and β_{224} to be 0.040 d^{-1} and 0.156 d^{-1}, respectively. It should be noted that the parameter β is in the same dimension with decay constant of radium isotopes (Su et al., 2013a). The results revealed that there were β_{223} and β_{224} both lower than the decay constant of ^{223}Ra (0.059 7 d^{-1}) and ^{224}Ra (0.189 d^{-1}), indicating that benthic radium flux played relatively fewer contributions to the radium activity in surface seawater compared to decay and water mixing (Moore, 2000). Furthermore, this study conducted an estimation based on β_{223} and β_{224}, considering the influence of benthic radium flux. By applying Eq. (2), this study obtained eddy diffusivity K_h of 2.1×10^8 cm^2/s

Table 1. All the parameters were applied to estimate SGD based on ^{224}Ra in the Subei Shoal

Parameter	Definition	Value	Reference
A/m^2	area of the study region	1.6×10^{10}	this study
V/m^3	water volume of the study region	1.9×10^{11}	this study
F_{riv}/(m^3·d^{-1})	freshwater discharge of rivers	3.0×10^7	Ma et al. (2010)
F_{sed}/(Bq·m^{-2}·d^{-1})	diffusion rate from sediment	20	Liu et al. (2018)
τ/d	water residence time	9.4[a]	this study
C_{SPM}/(g·m^{-3})	concentration of SPM in seawater	153	Zhao et al. (2018)
C_{SW}/(Bq·m^{-3})	^{224}Ra activity in seawater	10.7	this study
C_{ocean}/(Bq·m^{-3})	^{224}Ra activity in open Yellow Sea	0.20	Su et al. (2013b)
C_{riv}/(Bq·m^{-3})	^{224}Ra activity in river water	32.5[b]	this study
C_{des}/(Bq·g^{-1})	desorbed ^{224}Ra activity from SPM	0.023	Liu et al. (2018)
C_{GW}/(Bq·m^{-3})	^{224}Ra activity in coastal groundwater	81.2[c]	this study
F_{SGD}/(m^3·d^{-1})	SGD flux in the Subei Shoal	2.6×10^9	this study
SGD rate/(cm·d^{-1})	SGD rate normalized by area	16	this study

Note: a, Calculated by ^{224}Ra/^{223}Ra activity ratios based on the method in Liu et al. (2018); b, used the sample at a salinity of 20.9 as the riverine endmember to estimate the ^{224}Ra flux from both dissolved and desorbed components; c, referred to the maximum ^{224}Ra activity in coastal groundwater.

Table 2. Parameters for estimating eddy diffusivity mixing coefficient and advection rate in the Subei Shoal

	^{224}Ra slope/km^{-1}	R^2	^{223}Ra slope/km^{-1}	R^2	K_h/(cm^2·s^{-1})	w_x/(m·s^{-1})
Total data	−0.018 6	0.80	−0.015 4	0.76	2.3×10^8	−0.31
Transect SF	−0.018 5	0.92	−0.015 3	0.88	2.3×10^8	−0.31
Transect SE	−0.019 8	0.96	−0.017 4	0.81	3.0×10^8	−0.47
Transect SD	−0.017 6	0.94	−0.011 2	0.84	9.8×10^7	−0.05
Transect SC	−0.018 2	0.97	−0.013 4	0.78	1.4×10^8	−0.14
Transect SB	−0.020 6	0.92	−0.018 8	0.83	3.9×10^8	−0.69

and w_x advection of –0.29 m/s, which was comparable to the results under the assumption of no benthic radium flux, suggesting the availability of using Eq. (2) to calculate the eddy diffusivity in the Subei Shoal of this study. Additionally, this study calculated offshore eddy diffusivity K_h exceeded advection by several orders of magnitude, which the average K_h : w_x ratio of 100 km, suggesting that the ^{223}Ra and ^{224}Ra activities in surface seawater were mainly controlled by decay and dilution rather than advection (Moore, 2000; Sippo et al., 2019).

Due to the different hydrological environments, eddy diffusivity K_h varies considerably in different places, and covers a wide range (Su, 2013). In previous study, Men et al. (2006) estimated horizontal eddy diffusion coefficient at 2.9 × 10^7 cm^2/s based on ^{228}Ra within 200 km offshore in the western Yellow Sea, north of the study area. Then Su et al. (2013b) combined ^{223}Ra and ^{226}Ra, and obtained offshore K_h to be 3.7 × 10^7 cm^2/s within 500 km offshore in the Yellow Sea. Compared to these results, the estimated K_h (2.3 × 10^8 cm^2/s) was almost an order of magnitude higher. In the Subei Shoal, the surrounding irrigation canals and rivers deliver freshwater into the study area, although the discharge flux is relatively small (Ma et al., 2010) and not even reflected in the distribution of salinity (Fig. 2a), it may contribute to offshore transport of water mixing and elevate eddy diffusivity (Zhu and Wu, 2018). Additionally, a high tidal range of average at 4 m occurs in the Subei Shoal, which could also influence eddy diffusivity (Ding et al., 2014; Sippo et al., 2019). Here, this study summarized the eddy diffusivities estimated by ^{223}Ra and ^{224}Ra from different tidal ranges and scales (distance offshore), the results showed that eddy diffusion was higher when the study regions in higher tidal ranges and greater scales (Fig. 6), and similar relationship between eddy diffusion and distance offshore were also examined in previous studies (Dulaiova et al., 2009; Gómez-Álvarez et al., 2019; Su, 2013). Therefore, the eddy diffusivity K_h estimated in this study was reasonable and could be applied to calculate the nutrient fluxes in the following discussion.

4.2 *Nutrient outwelling fluxes*

In general, SGD and eddy diffusion are not only simple water movements, more importantly, they also carry a large amount of dissolved chemicals transporting (Sippo et al., 2019; Su et al., 2013a; Zhang et al., 2020a). The widely used method for determining nutrient flux transported from SGD is to multiple the SGD flux by the difference of nutrient concentrations between coastal groundwater and nearshore seawater (Liu et al., 2019; Wang et al., 2015). This study chose the average nutrient concentrations of seawater within 60 km from the shoreline as the nearshore seawater endmember, resulting in nutrient concentrations in SGD endmember were 31 μmol/L, 0.61 μmol/L and 104 μmol/L for DIN, DIP and DSi, respectively. Therefore, the nutrient fluxes transported from SGD were obtained to be 8.1×10^7 mol/d for DIN, 1.6×10^6 mol/d for DIP and 2.2×10^8 mol/d for DSi, which were comparable with the results reported in Zhao et al. (2018) of the Subei Shoal. Given that such fluxes of nutrient outwelling from the Subei Shoal could be distributed evenly over the Yellow Sea, which covers an area of 3.09 × 10^{11} m^2, the normalized nutrient fluxes via SGD would be 262 μmol/(m^2·d), 5.2 μmol/(m^2·d) and 711 μmol/(m^2·d) for DIN, DIP and DSi, respectively (Fig. 7).

The nutrient outwelling derived by eddy diffusion was calcu-

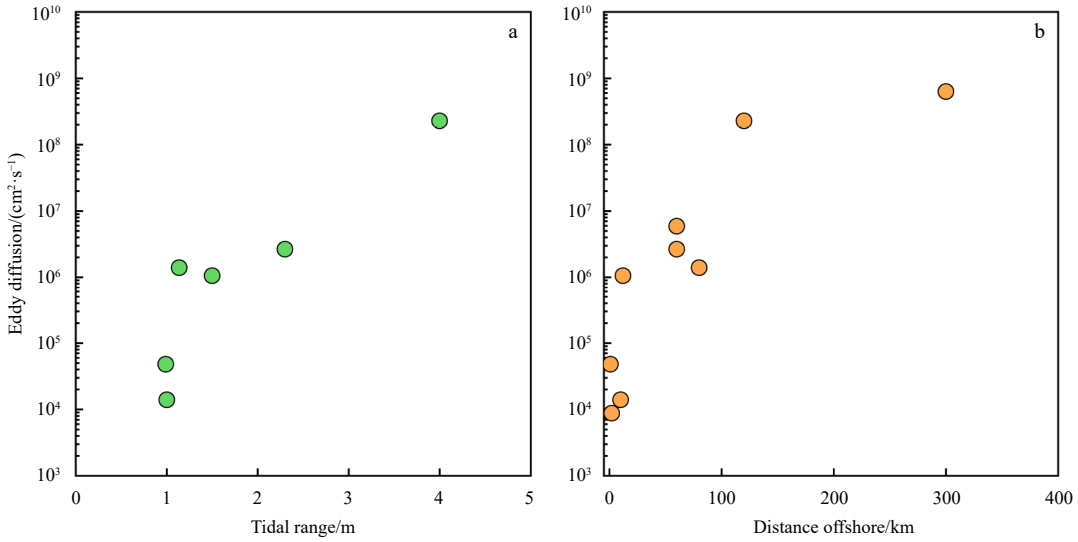

Fig. 6. The summarized relationship between ^{223}Ra- and ^{224}Ra-derived eddy diffusion and tidal range (a), ^{223}Ra- and ^{224}Ra-derived eddy diffusion and distance offshore (b). Date cited from Annett et al. (2013); Colbert and Hammond (2007); Dulaiova et al. (2009); Gómez-Álvarez et al. (2019); Hancock et al. (2006); Sippo et al. (2019) and Stachelhaus and Moran (2012).

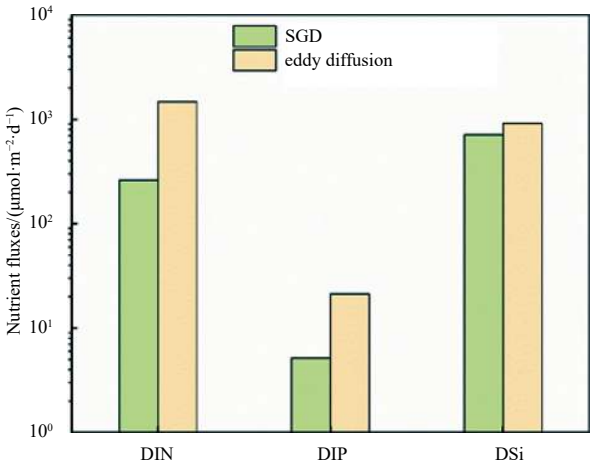

Fig. 7. Nutrient outwelling fluxes from eddy diffusion and SGD-derived nutrient fluxes from the Subei Shoal to the Yellow Sea.

lated by multiplying the linear gradients of DIN, DIP and DSi by the eddy diffusivity mixing coefficient, which has been widely applied in previous studies (Moore, 2000; Santos et al., 2008; Sippo et al., 2019). From Fig. 5, significant offshore nutrient gradients were observed in the Subei Shoal, and those were 0.248 3 μmol/(L·km) for DIN, 0.003 6 μmol/(L·km) for DIP and 0.154 8 μmol/(L·km) for DSi. Here, this study used the average mixing coefficient, calculated from all data and combined five individual transects, of 2.3×10^8 cm²/s. Besides, considering the coastline covered of 183 km and the mean well-mixed layer depth of 5 m in the study area of the Subei Shoal (Cheng et al., 2017; Zhou et al., 2008), DIN, DIP and DSi outwelling into the Yellow Sea were estimated to be 1 465 μmol/(m²·d), 21 μmol/(m²·d) and 913 μmol/(m²·d), respectively (Fig. 7).

As a result, combined these two pathways of SGD and eddy diffusion, the nutrient outwelling fluxes from the Subei Shoal to the Yellow Sea were determined to be 262–1 465 μmol/(m²·d), 5.2–21.0 μmol/(m²·d) and 711–913 μmol/(m²·d) for DIN, DIP and DSi, respectively (Fig. 7). In previous studies, the traditional external sources for nutrient in the Yellow Sea were known from surrounding rivers and atmospheric deposition (Liu et al., 2003), in which rivers could provide 212 μmol/(m²·d) DIN, 3.3 μmol/(m²·d) DIP and 142 μmol/(m²·d) DSi (Liu et al., 2009b), and atmospheric deposition supplied 99 μmol/(m²·d) DIN, 1.6 μmol/(m²·d) DIP and 3.8 μmol/(m²·d) DSi (Zhang et al., 2007b). This comparison suggested that nutrient outwelling fluxes from the Subei Shoal were approximately 1–7 times higher than the riverine inputs and atmospheric deposition. In addition, the discharge of mariculture was also recognized as a considerable external source of nutrient to the Yellow Sea, which was reported to be 5.8 μmol/(m²·d) and 0.10 μmol/(m²·d) for DIN and DSi, respectively (Li et al., 2015). Therefore, this study could conclude that the nutrient outwelling from the Subei Shoal was the dominant nutrient source (Fig. 8), and have the potential to affect the biogeochemical cycles in the Yellow Sea. It should be noted that the obtained nutrient outwelling fluxes to the Yellow Sea were overestimated, because this study did the calculations without considering the influence of biological uptake and scavenge on nutrient cycles in the seawater (Charette et al., 2007; Su et al., 2013b). Nevertheless, the results could also shed light on potential environmental impacts of nutrient outwelling via SGD and eddy diffusion from coastal waters.

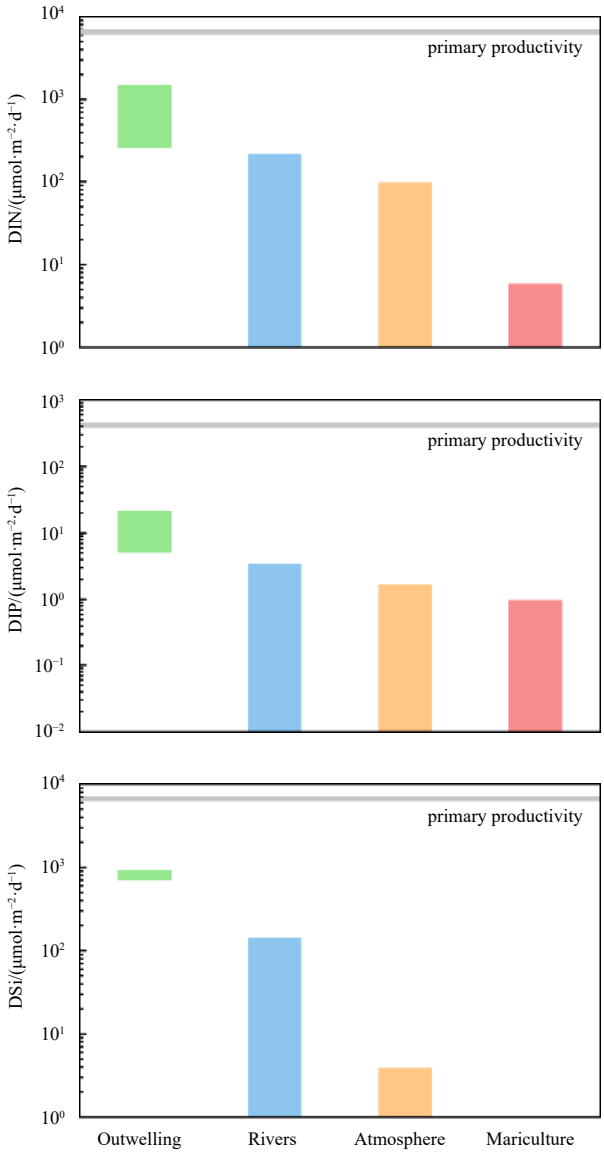

Fig. 8. Fluxes of nutrients to the Yellow Sea derived by outwelling, riverine inputs, atmospheric deposition and mariculture. Gray lines indicate the average nutrient-supported primarily productivity in the Yellow Sea (Jin et al., 2013). DSi flux from mariculture was unavailable.

4.3 *Environmental implications*

With the rapid development of mariculture and significant terrestrial materials input, the Subei Shoal was recognized as the hot spot for nutrient enrichment, and the high concentrations of nutrient often occur in the nearshore water of the Subei Shoal (Li et al., 2015; Shi et al., 2015). In such a case, the high nutrient supply, especially DIN and DIP, supported the Subei Shoal became the originating area of green tides bloom (Li et al., 2017; Liu et al., 2013). Meanwhile, along with the water movement, nutrient in the Subei Shoal may transport to the Yellow Sea basin and then influence its ecological environment. It was reported that the assimilated nutrient fluxes for supporting phytoplankton growth in the Yellow Sea were 6 350 μmol/(m²·d) for N and 400 μmol/(m²·d) for P on average (Fig. 8) (Jin et al., 2013). Assuming that nutrient outwelling fluxes from the Subei Shoal were bioavailable and assimilated by phytoplankton, the nutrient fluxes could contribute

to 4.1%–23% N and 1.3%–5.3% P for the primary productivity in the Yellow Sea, revealing that the nutrient outwelling played an important role in maintaining phytoplankton primary production in the Yellow Sea. Meanwhile, it is clearly observed that the recognized DIN and DIP fluxes could not meet the nutrient demand for phytoplankton growth in the Yellow Sea, suggesting that there should be other nutrient sources to balance the requirements, such as benthic fluxes and regeneration and recycling of nutrient (Liu et al., 2003; Ziegler and Benner, 1999). For instance, *Ulva prolifera*, known as green tides, could also assimilate dissolved organic nitrogen (DON) and phosphorus (DOP) directly (Shi et al., 2015), and that SGD and eddy diffusion transport DON and DOP from the Subei Shoal are known now, further confirming the significance of the nutrient outwelling.

More importantly, this study found that nutrient outwelling from the Subei Shoal not only could contribute to nutrient budgets in the Yellow Sea, but also may alter the nutrient structures. In the seawater of the Yellow Sea, the stoichiometric ratios of DIN/DIP and DSi/DIP were observed to be 17–40 and 27–47, respectively (Jin et al., 2013; Shi et al., 2015), which deviated from the Redfield ratio of 16, indicating a P limitation condition in the Yellow Sea. This study noticed that DIN/DIP ratios in nutrient outwelling were 50–69 and much higher than the Redfield ratio by a factor of 3–4. Therefore, large nutrient fluxes with deviated DIN/DIP ratio outwelling from the Subei Shoal were bound to aggravate the P limitation and probably affect the eco-environment of the Yellow Sea.

5 Conclusions

Because of the application limitations of ^{226}Ra and ^{228}Ra in the coastal waters, ^{223}Ra and ^{224}Ra are more suitable for calculating the water mixing processes in the Subei Shoal. This study demonstrates the applications of ^{223}Ra and ^{224}Ra in obtaining the offshore eddy diffusivity mixing coefficient in the Subei Shoal, as well as SGD. The results reveal that the nutrient outwelling fluxes from the Subei Shoal not only contribute to the nutrient budgets and phytoplankton primary production, but also affect the nutrient structures in the Yellow Sea. These large amounts of nutrient outwelling fluxes from the Subei Shoal may contribute to the development of the green tides bloom in the Yellow Sea, however, more robust and in-depth research in the future are warranted.

Acknowledgements

We thank Captain Lin Wei and the crew on R/V *SURUYUYUN-288* for their assistance in the sample collection. We thank Wanli Xing and Qian Ma from SKLEC/ECNU for their help in field observations.

References

Andersen J H, Conley D J. 2009. Eutrophication in coastal marine ecosystems: towards better understanding and management strategies. Hydrobiologia, 629(1): 1–4, doi: 10.1007/s10750-009-9758-0

Anderson D M, Glibert P M, Burkholder J M. 2002. Harmful algal blooms and eutrophication: nutrient sources, composition, and consequences. Estuaries, 25(4B): 704–726, doi: 10.1007/bf02804901

Annett A L, Henley S F, Van Beek P, et al. 2013. Use of radium isotopes to estimate mixing rates and trace sediment inputs to surface waters in northern Marguerite Bay, Antarctic Peninsula. Antarctic Science, 25(3): 445–456, doi: 10.1017/s0954102012000892

Bao Min, Guan Weibing, Wang Zongling, et al. 2015. Features of the physical environment associated with green tide in the southwestern Yellow Sea during spring. Acta Oceanologica Sinica, 34(7): 97–104, doi: 10.1007/s13131-015-0692-x

Charette M A, Gonneea M E, Morris P J, et al. 2007. Radium isotopes as tracers of iron sources fueling a Southern Ocean phytoplankton bloom. Deep-Sea Research Part II: Topical Studies in Oceanography, 54(18–20): 1989–1998, doi: 10.1016/j.dsr2.2007.06.003

Cheng Xueli, Sun Qun, Wang Yuheng, et al. 2017. Analysis on seasonal variations and structures of the tidal front outside of the Subei Shoal. Marine Sciences, 41(12): 1–8, doi: 10.11759/hykx20151108001

Colbert S L, Hammond D E. 2007. Temporal and spatial variability of radium in the coastal ocean and its impact on computation of nearshore cross-shelf mixing rates. Continental Shelf Research, 27(10–11): 1477–1500, doi: 10.1016/j.csr.2007.01.003

Ding Xianrong, Kang Yanyan, Mao Zhibing, et al. 2014. Analysis of largest tidal range in radial sand ridges southern Yellow Sea. Haiyang Xuebao (in Chinese), 36(11): 12–20, doi: 10.3969/j.issn.0253-4193.2014.11.002

Dulaiova H, Ardelan M V, Henderson P B, et al. 2009. Shelf-derived iron inputs drive biological productivity in the southern Drake Passage. Global Biogeochemical Cycles, 23(4): GB4014, doi: 10.1029/2008gb003406

Falkowski P G, Barber R T, Smetacek V. 1998. Biogeochemical controls and feedbacks on ocean primary production. Science, 281(5374): 200–206, doi: 10.1126/science.281.5374.200

Fischer H B. 1980. Mixing processes on the Atlantic continental shelf, Cape Cod to Cape Hatteras. Limnology and Oceanography, 25(1): 114–125, doi: 10.4319/lo.1980.25.1.0114

Garcia-Orellana J, Cochran J K, Bokuniewicz H, et al. 2014. Evaluation of ^{224}Ra as a tracer for submarine groundwater discharge in Long Island Sound (NY). Geochimica et Cosmochimica Acta, 141: 314–330, doi: 10.1016/j.gca.2014.05.009

Garcia-Solsona E, Garcia-Orellana J, Masqué P, et al. 2008. Uncertainties associated with ^{223}Ra and ^{224}Ra measurements in water via a Delayed Coincidence Counter (RaDeCC). Marine Chemistry, 109(3–4): 198–219, doi: 10.1016/j.marchem.2007.11.006

Gómez-Álvarez P, Bates B, Santos I R, et al. 2019. Submarine groundwater discharge revealed by ^{224}Ra and ^{223}Ra in Coffs Harbour, Australia. Journal of Radioanalytical and Nuclear Chemistry, 319(3): 1193–1199, doi: 10.1007/s10967-019-06412-0

Gu Hequan. 2015. A quantitative study on the sources and sinks of radium isotopes in near-shore waters—Taking Changjiang estuary and its adjacent offshore area, Bamen Lagoon, Gaolong Bay and Boao Bay in Hainan for example (in Chinese) [dissertation]. Shanghai: East China Normal University

Hancock G J, Webster I T, Stieglitz T C. 2006. Horizontal mixing of Great Barrier Reef waters: offshore diffusivity determined from radium isotope distribution. Journal of Geophysical Research, 111(C12): C12019, doi: 10.1029/2006jc003608

Jin Jie, Liu Sumei, Ren Jingling, et al. 2013. Nutrient dynamics and coupling with phytoplankton species composition during the spring blooms in the Yellow Sea. Deep-Sea Research Part Ⅱ: Topical Studies in Oceanography, 97: 16–32, doi: 10.1016/j.dsr2.2013.05.002

Ku T L, Luo Shangde. 1994. New appraisal of Radium 226 as a large-scale oceanic mixing tracer. Journal of Geophysical Research, 99(C5): 10255–10273, doi: 10.1029/94JC00089

Kwon H K, Kim G, Han Yongjin, et al. 2019. Tracing the sources of nutrients fueling dinoflagellate red tides occurring along the coast of Korea using radium isotopes. Scientific Reports, 9(1): 15319, doi: 10.1038/s41598-019-51623-w

Le Moal M, Gascuel-Odoux C, Ménesguen A, et al. 2019. Eutrophication: a new wine in an old bottle?. Science of the Total Environment, 651: 1–11, doi: 10.1016/j.scitotenv.2018.09.139

Li Chunyan, Cai Weijun. 2011. On the calculation of eddy diffusivity in the shelf water from radium isotopes: high sensitivity to advection. Journal of Marine Systems, 86(1–2): 28–33, doi: 10.1016/j.jmarsys.2011.01.003

Li Yuanhui, Mathieu G, Biscaye P, et al. 1977. The flux of ^{226}Ra from estuarine and continental shelf sediments. Earth and Planetary

Science Letters, 37(2): 237–241, doi: 10.1016/0012-821X(77)90168-6

Li Hongmei, Zhang Chuansong, Han Xiurong, et al. 2015. Changes in concentrations of oxygen, dissolved nitrogen, phosphate, and silicate in the southern Yellow Sea, 1980–2012: sources and seaward gradients. Estuarine, Coastal and Shelf Science, 163: 44–55, doi: 10.1016/j.ecss.2014.12.013

Li Hongmei, Zhang Yongyu, Tang Hongjie, et al. 2017. Spatiotemporal variations of inorganic nutrients along the Jiangsu coast, China, and the occurrence of macroalgal blooms (green tides) in the southern Yellow Sea. Harmful Algae, 63: 164–172, doi: 10.1016/j.hal.2017.02.006

Liu Jianan, Du Jinzhou, Wu Ying, et al. 2018. Nutrient input through submarine groundwater discharge in two major Chinese estuaries: the Pearl River Estuary and the Changjiang River Estuary. Estuarine, Coastal and Shelf Science, 203: 17–28, doi: 10.1016/j.ecss.2018.02.005

Liu Sumei, Hong G H, Zhang Jing, et al. 2009b. Nutrient budgets for large Chinese estuaries. Biogeosciences, 6(10): 2245–2263, doi: 10.5194/bg-6-2245-2009

Liu Jianan, Hrustić E, Du Jinzhou, et al. 2019. Net submarine groundwater-derived dissolved inorganic nutrients and carbon input to the oligotrophic stratified karstic estuary of the Krka River (Adriatic Sea, Croatia). Journal of Geophysical Research, 124(6): 4334–4349, doi: 10.1029/2018jc014814

Liu Dongyan, Keesing J K, He Peimin, et al. 2013. The world's largest macroalgal bloom in the Yellow Sea, China: formation and implications. Estuarine, Coastal and Shelf Science, 129: 2–10, doi: 10.1016/j.ecss.2013.05.021

Liu Dongyan, Keesing J K, Xing Qianguo, et al. 2009a. World's largest macroalgal bloom caused by expansion of seaweed aquaculture in China. Marine Pollution Bulletin, 58(6): 888–895, doi: 10.1016/j.marpolbul.2009.01.013

Liu Jian'an, Su Ni, Wang Xilong, et al. 2017. Submarine groundwater discharge and associated nutrient fluxes into the southern Yellow Sea: a case study for semi-enclosed and oligotrophic seas-implication for green tide bloom. Journal of Geophysical Research, 122(1): 139–152, doi: 10.1002/2016jc012282

Liu Xiangqing, Wang Zongling, Zhang Xuelei. 2016. A review of the green tides in the Yellow Sea, China. Marine Environmental Research, 119: 189–196, doi: 10.1016/j.marenvres.2016.06.004

Liu Sumei, Zhang Jing, Chen S Z, et al. 2003. Inventory of nutrient compounds in the Yellow Sea. Continental Shelf Research, 23(11–13): 1161–1174, doi: 10.1016/S0278-4343(03)00089-X

Ma Hongrui, Chen Jufa, Cui Yi, et al. 2010. Analysis of water quality and assessment of major pollutants input to the sea from the Guan River and Sheyang River. Progress in Fishery Sciences, 31(3): 92–99

Men Wu, Wei Hao, Liu Guangshan. 2006. ^{226}Ra and ^{228}Ra in the seawater of the western Yellow Sea. Journal of Ocean University of China, 5(3): 228–234, doi: 10.1007/s11802-006-0006-1

Miao Xiaoxiang, Xiao Jie, Xu Qinzeng, et al. 2020. Distribution and species diversity of the floating green macroalgae and micropropagules in the Subei Shoal, southwestern Yellow Sea. PeerJ, 8: e10538, doi: 10.7717/peerj.10538

Moore W S. 1976. Sampling ^{228}Ra in the deep ocean. Deep Sea Research and Oceanographic Abstracts, 23(7): 647–651, doi: 10.1016/0011-7471(76)90007-3

Moore W S. 1996. Large groundwater inputs to coastal waters revealed by ^{226}Ra enrichments. Nature, 380(6575): 612–614, doi: 10.1038/380612a0

Moore W S. 2000. Determining coastal mixing rates using radium isotopes. Continental Shelf Research, 20(15): 1993–2007, doi: 10.1016/S0278-4343(00)00054-6

Moore W S. 2008. Fifteen years experience in measuring ^{224}Ra and ^{223}Ra by delayed-coincidence counting. Marine Chemistry, 109(3–4): 188–197, doi: 10.1016/j.marchem.2007.06.015

Moore W S. 2010. The effect of submarine groundwater discharge on the ocean. Annual Review of Marine Science, 2: 59–88, doi: 10.1146/annurev-marine-120308-081019

Moore W S. 2015. Inappropriate attempts to use distributions of ^{228}Ra and ^{226}Ra in coastal waters to model mixing and advection rates. Continental Shelf Research, 105: 95–100, doi: 10.1016/j.csr.2015.05.014

Moore W S, Arnold R. 1996. Measurement of ^{223}Ra and ^{224}Ra in coastal waters using a delayed coincidence counter. Journal of Geophysical Research, 101(C1): 1321–1329, doi: 10.1029/95jc03139

Pasquero C. 2005. Differential eddy diffusion of biogeochemical tracers. Geophysical Research Letters, 32(17): L17603, doi: 10.1029/2005gl023662

Santos I R, Niencheski F, Burnett W, et al. 2008. Tracing anthropogenically driven groundwater discharge into a coastal lagoon from southern Brazil. Journal of Hydrology, 353(3–4): 275–293, doi: 10.1016/j.jhydrol.2008.02.010

Sarmiento J L, Thiele G, Key R M, et al. 1990. Oxygen and nitrate new production and remineralization in the North Atlantic subtropical gyre. Journal of Geophysical Research, 95(C10): 18303–18315, doi: 10.1029/JC095iC10p18303

Shi Xiaoyong, Qi Mingyan, Tang Hongjie, et al. 2015. Spatial and temporal nutrient variations in the Yellow Sea and their effects on *Ulva prolifera* blooms. Estuarine, Coastal and Shelf Science, 163: 36–43, doi: 10.1016/j.ecss.2015.02.007

Sippo J Z, Maher D T, Schulz K G, et al. 2019. Carbon outwelling across the shelf following a massive mangrove dieback in Australia: insights from radium isotopes. Geochimica et Cosmochimica Acta, 253: 142–158, doi: 10.1016/j.gca.2019.03.003

Stachelhaus S L, Moran S B. 2012. A simple differential diffusion model to account for the discrepancy between ^{223}Ra- and ^{224}Ra-based eddy diffusivities. Journal of Geophysical Research, 117(C3): C03004, doi: 10.1029/2011jc007500

Su Ni. 2013. Tracing coastal water mixing processes and submarine groundwater discharge by radium isotopes (in Chinese) [dissertation]. Shanghai: East China Normal University

Su Ni, Du Jinzhou, Li Ying, et al. 2013a. Evaluation of surface water mixing and associated nutrient fluxes in the East China Sea using ^{226}Ra and ^{228}Ra. Marine Chemistry, 156: 108–119, doi: 10.1016/j.marchem.2013.04.009

Su Ni, Du Jinzhou, Liu Sumei, et al. 2013b. Nutrient fluxes via radium isotopes from the coast to offshore and from the seafloor to upper waters after the 2009 spring bloom in the Yellow Sea. Deep-Sea Research Part II: Topical Studies in Oceanography, 97: 33–42, doi: 10.1016/j.dsr2.2013.05.003

Swarzenski P W. 2007. U/Th series radionuclides as coastal groundwater tracers. Chemical Reviews, 107(2): 663–674, doi: 10.1021/cr0503761

Tang Danling, Kawamura H, Doan-Nhu H, et al. 2004. Remote sensing oceanography of a harmful algal bloom off the coast of southeastern Vietnam. Journal of Geophysical Research, 109(C3): C03014, doi: 10.1029/2003jc002045

Walsh J J. 1991. Importance of continental margins in the marine biogeochemical cycling of carbon and nitrogen. Nature, 350(6313): 53–55, doi: 10.1038/350053a0

Wang Xuejing, Li Hailong, Zheng Chunmiao, et al. 2018. Submarine groundwater discharge as an important nutrient source influencing nutrient structure in coastal water of Daya Bay, China. Geochimica et Cosmochimica Acta, 225: 52–65, doi: 10.1016/j.gca.2018.01.029

Wang Guizhi, Wang Zhangyong, Zhai Weidong, et al. 2015. Net subterranean estuarine export fluxes of dissolved inorganic C, N, P, Si, and total alkalinity into the Jiulong River estuary, China. Geochimica et Cosmochimica Acta, 149: 103–114, doi: 10.1016/j.gca.2014.11.001

Werner F E, Blanton J O, Lynch D R, et al. 1993. A numerical study of the continental shelf circulation of the U. S. South Atlantic Bight during the autumn of 1987. Continental Shelf Research, 13(8–9): 971–997, doi: 10.1016/0278-4343(93)90019-t

Xiao Jie, Fan Shiliang, Wang Zongling, et al. 2020. Decadal characteristics of the floating *Ulva* and *Sargassum* in the Subei Shoal, Yellow Sea. Acta Oceanologica Sinica, 39(10): 1–10, doi: 10.1007/s13131-020-1655-4

Zhang Jing, Liu Sumei, Ren Jingling, et al. 2007a. Nutrient gradients from the eutrophic Changjiang (Yangtze River) Estuary to the oligotrophic Kuroshio waters and re-evaluation of budgets for the East China Sea Shelf. Progress in Oceanography, 74(4): 449–478, doi: 10.1016/j.pocean.2007.04.019

Zhang Yan, Santos I R, Li Hailong, et al. 2020a. Submarine groundwater discharge drives coastal water quality and nutrient budgets at small and large scales. Geochimica et Cosmochimica Acta, 290: 201–215, doi: 10.1016/j.gca.2020.08.026

Zhang Haibo, Su Rongguo, Shi Xiaoyong, et al. 2020b. Role of nutrients in the development of floating green tides in the Southern Yellow Sea, China, in 2017. Marine Pollution Bulletin, 156: 111197, doi: 10.1016/j.marpolbul.2020.111197

Zhang Guosen, Zhang Jing, Liu Sumei. 2007b. Characterization of nutrients in the atmospheric wet and dry deposition observed at the two monitoring sites over Yellow Sea and East China Sea. Journal of Atmospheric Chemistry, 57(1): 41–57, doi: 10.1007/s10874-007-9060-3

Zhao Shibin, Yao Qingzhen, Yu Zhigang, et al. 2018. Submarine groundwater discharge and its contribution to nutrients fluxes in the Subei Shoal, China. Oceanologia et Limnologia Sinica, 49(5): 1038–1044

Zhou Feng, Huang Daji, Wang Ruijing, et al. 2008. Observations and analysis of tidal fronts in the southwestern Huanghai Sea. Haiyang Xuebao (in Chinese), 30(3): 9–15

Zhu Ping, Wu Hui. 2018. Origins and transports of the low-salinity coastal water in the southwestern Yellow Sea. Acta Oceanologica Sinica, 37(4): 1–11, doi: 10.1007/s13131-018-1200-x

Ziegler S, Benner R. 1999. Nutrient cycling in the water column of a subtropical seagrass meadow. Marine Ecology Progress Series, 188: 51–62, doi: 10.3354/meps188051